

Effect of recent R_p and R_n measurements on extended Gari-Krümpelmann model fits to nucleon electromagnetic form factors

Earle L. Lomon

Center for Theoretical Physics

Laboratory for Nuclear Science and Department of Physics

Massachusetts Institute of Technology,

Cambridge, Massachusetts 02139

MIT-CTP-3257

The Gari-Krümpelmann (GK) models of nucleon electromagnetic form factors, in which the ρ , ω , and ϕ vector meson pole contributions evolve at high momentum transfer to conform to the predictions of perturbative QCD (pQCD), was recently extended to include the width of the ρ meson by substituting the result of dispersion relations for the pole and the addition of the ρ' (1450) isovector vector meson pole. This extended model was shown to produce a good overall fit to all the available nucleon electromagnetic form factor (emff) data. Since then new polarization data shows that the electric to magnetic ratios R_p and R_n obtained are not consistent with the older G_{Ep} and G_{En} data in their range of momentum transfer. The model is further extended to include the ω' (1419) isoscalar vector meson pole. It is found that while this GKex cannot simultaneously fit the new R_p and the old G_{En} data, it can fit the new R_p and R_n well simultaneously. An excellent fit to all the remaining data is obtained when the inconsistent G_{Ep} and G_{En} is omitted. The model predictions are extended beyond the data, if needed, to momentum transfer squared, Q^2 , of 8 GeV^2/c^2 .

PACS numbers: 13.40.Gp, 21.10.Ft

I. INTRODUCTION

A variety of related models of the nucleon emff [1] were fitted to the complete set of data available before September 2001. One group of models included variants of the basic GK model of ρ , ω , and ϕ vector meson pole terms with hadronic form factors and a term with pQCD behavior which dominates at high Q^2 [2]. Four varieties of hadronic form factor parameterization (of which two are used in [2]) were compared. In addition to the GK type models we considered a group of models (generically designated DR-GK) that use the analytic approximation of [3] to the dispersion integral approximation for the ρ meson contribution (similar to that of [4]), modified by the four hadronic form factor choices used with the GK model, and the addition of the well established ρ' (1450) pole. Every model had an electric and a magnetic coupling parameter for each of the three pole terms, four “cut-off” masses for the hadronic form-factors and the QCD scale mass scale, Λ_{QCD} for the logarithmic momentum transfer behavior in pQCD. In addition the effect of a normalization parameter was sometimes considered for the dispersion relation behavior of the ρ meson in the DR-GK models.

When the set of parameters in each of the eight models was fitted to the full set of

data available before publication, for G_{Ep} , G_{Mp} , G_{En} , G_{Mn} and the lower Q^2 values of $R_p \equiv \mu_p G_{Ep}/G_{Mp}$, three GK and all four DR-GK models attained reasonable χ^2 (when the inconsistency of some low Q^2 G_{En} and G_{Mn} data was taken into account), but the extended DR-GK models had significantly lower χ^2 . Furthermore Λ_{QCD} was reasonable for three of the DR-GK models but for only the one of the GK models that had an unreasonably large anomalous magnetic coupling κ_ρ . It was concluded that the three DR-GK models were the best nucleon emff to use in prediction of nuclear electromagnetic properties. All three were found to be moderately consistent in their predictions up to Q^2 of 8 GeV^2/c^2 .

However the part of the above data set from a recent R_p ratio data [5] for $0.5 \text{ GeV}^2/c^2 \leq Q^2 \leq 3.5 \text{ GeV}^2/c^2$, swamped statistically by all the other data, was systematically lower than the fitted models (Fig.5 of [1]) contributing disproportionately to χ^2 . This ratio is determined by an asymmetry measurement in the scattering of polarized electrons on protons. Multiplied by the well determined values of G_{Mp} one obtains values for G_{Ep} which are not subject to the uncertainty inherent in the Rosenbluth separation measurements in which G_{Ep} is obtained by subtracting the much larger contribution of G_{Mp} from the unpolarized cross section. As expected the G_{Ep} derived from the measured R_p are consistently below those of the older Rosenbluth separation values.

It is plausible to expect that the old G_{Ep} data is responsible for restricting the best fit of the models to be substantially above the experimental R_p values. With this in mind the particularly high data of [6] was omitted from the fit to the model type DR-GK'(1) of [1] and the flexibility of a ρ meson dispersion integral normalization parameter N was included. In this article the original version is designated as GKex(01) and when fitted to the smaller data set as GKex(01-). As seen in Tables I and II and Figs. 1 and 2, there is only a small change in the fit to G_{Ep} and R_p , although the parameters of the fit change substantially.

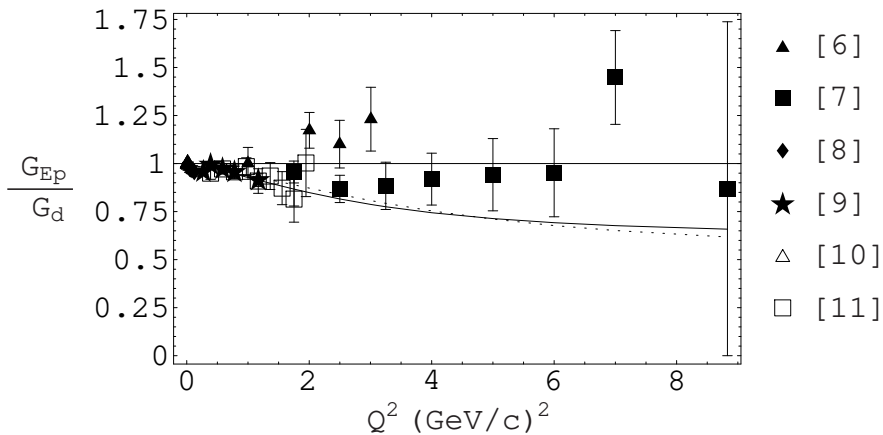


FIG. 1: G_{Ep} normalized to G_d , comparing the GKex(01) fit [dotted] with the fit GKex(01-) [solid] obtained when the data of [6] is omitted. The other G_{Ep} data is from [7], [8], [9], [10], and [11]. The data symbols are listed in the figure.

After the publication of [1] new data [13] extended the measurements of R_p up to $Q^2 = 5.6 \text{ GeV}^2/c^2$, exacerbating the discrepancy with the predictions of the best models in [1]. Very recently $R_n \equiv \mu_n G_{En}/G_{Mn}$ has been obtained directly [14] by the scattering of polarized electrons on deuterium and detecting the polarized recoil neutron at $Q^2 = 0.45, 1.15$ and

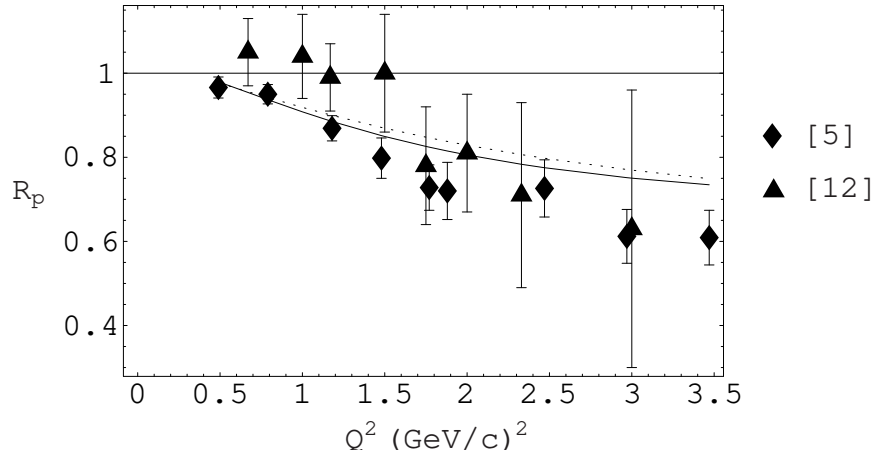


FIG. 2: R_p , the ratio $\mu_p G_{Ep}/G_{Mp}$, comparing the GKex(01) fit [dotted] with the fit GKex(01-) [solid] obtained when the data of [6] is omitted. The data is from [5] and [12]. The data symbols are listed in the figure.

1.47 GeV^2/c^2 . The preliminary results are consistent with the Galster [15] parameterization from lower Q^2 data

$$R_n^{Galster}(Q^2) = -\frac{\mu_n \tau}{1 + 5.6\tau}, \quad \tau = \frac{Q^2}{4m_N^2}. \quad (1)$$

which, in parallel to the situation for R_p , implies much lower values of G_{En} in their Q^2 range when coupled with G_{Mn} values (either the precision data of [16] or the model fits).

In this paper, in addition to the above comparison of GKex(01) and GKex(01-), we fit the model of type DR-GK'(1), with the added isoscalar vector meson $\omega'(1419)$ pole, to the following data sets, chosen to determine the effect of the old G_{En} and G_{Ep} data in direct conflict with the values of R_n and R_p from modern polarization measurements:

- (a) The fit GKex(02L) from the full data set of [1] with the addition of [13] and [14], the omission of [6] (as above for GKex(01-)) and the G_{En} values for $Q^2 \geq 0.779 \text{ GeV}^2/c^2$ of [9], [17], and [18].
- (b) The fit of GKex(02S) to the same data set as above except for the omission of the G_{Ep} values for $Q^2 \geq 1.75 \text{ GeV}^2/c^2$ of [7].

It will be seen that the omission of the conflicting G_{En} data, GKex(02L), has a much bigger influence than the omission of [6], GKex(01-), enabling a much better fit to R_p in addition to a very good fit to R_n , compared to GKex(01). With the removal of the conflicting G_{Ep} data, GKex(02S), the fit to all the remaining data, including R_p , is very satisfactory.

In Section II we will specify the models and parameters used in this article, and the data sets used in Section III. In Section IV we present the results of the four GKex fits in comparison with each other. We extrapolate beyond the present experimental range of momentum transfer where necessary for predicting available deuteron emff data. The model GKex(02S) fits the modern and consistent older data well and meets the requirements of dispersion relations and of QCD at low and high momentum transfer. Conclusions are presented in Section V.

II. THE NUCLEON EMFF MODEL

In fitting the nucleon emff data including the new R_n and R_p results we have chosen to use the extended GK model DR-GK'(1) of Ref. [1] with the addition of a pole term for the well established isoscalar vector meson $\omega'(1419)$, whose mass is lower than that of the already included isovector vector meson $\rho'(1450)$. We denote this model as GKex. The choice of the particular parameterization DR-GK'(1) was made because of its low χ^2 value and the fact that its predicted values of R_p were a little closer to the data than those of the other extended models. In addition DR-GK'(1) has the following good physical properties:

- (1) It uses the QCD cut-off Λ_2 for the helicity flip meson-nucleon form factors, rather than the meson cut-off Λ_1 used by DR-GK(3) and DR-GK'(3).
- (2) The evolution of the logarithmic dependence on Q^2 is controlled by the quark-nucleon cut-off Λ_D , along with Λ_{QCD} . DR-GK(1) and DR-GK(3) use Λ_2 instead of Λ_D .
- (3) Fitted to the data set of [1] it finds $\Lambda_{\text{QCD}} = .1163$, close to the expected value. The form factors are not very sensitive to this parameter which is fixed at .15 for the fits to the new data sets.

So that the reader need not make constant reference to [1] we repeat the relevant formulas here together with the new $\omega'(1419)$ terms.

The emff of a nucleon are defined by the matrix elements of the electromagnetic current J_μ

$$\langle N(p') | J_\mu | N(p) \rangle = e \bar{u}(p') \left\{ \gamma_\mu F_1^N(Q^2) + \frac{i}{2m_N} \sigma_{\mu\nu} Q^\nu F_2^N(Q^2) \right\} u(p) \quad (2)$$

where N is the neutron, n , or proton, p , and $-Q^2 = (p' - p)^2$ is the square of the invariant momentum transfer. $F_1^N(Q^2)$ and $F_2^N(Q^2)$ are respectively the Dirac and Pauli form factors, normalized at $Q^2 = 0$ as

$$F_1^p(0) = 1, \quad F_1^n(0) = 0, \quad F_2^p(0) = \kappa_p, \quad F_2^n(0) = \kappa_n. \quad (3)$$

The Sachs form factors, most directly obtained from experiment, are then

$$\begin{aligned} G_{\text{EN}}(Q^2) &= F_1^N(Q^2) - \tau F_2^N(Q^2) \\ G_{\text{MN}}(Q^2) &= F_1^N(Q^2) + F_2^N(Q^2). \end{aligned} \quad (4)$$

Expressed in terms of the isoscalar and isovector electromagnetic currents

$$2F_i^p = F_i^{is} + F_i^{iv}, \quad 2F_i^n = F_i^{is} - F_i^{iv}, \quad (i = 1, 2). \quad (5)$$

The GKex model has the following form for the four isotopic emff:

$$\begin{aligned}
F_1^{iv}(Q^2) &= N/2 \frac{1.0317 + 0.0875(1 + Q^2/0.3176)^{-2}}{(1 + Q^2/0.5496)} F_1^\rho(Q^2) \\
&\quad + \frac{g_{\rho'}}{f_{\rho'}} \frac{m_{\rho'}^2}{m_{\rho'}^2 + Q^2} F_1^\rho(Q^2) + \left(1 - 1.1192 N/2 - \frac{g_{\rho'}}{f_{\rho'}}\right) F_1^D(Q^2) \\
F_2^{iv}(Q^2) &= N/2 \frac{5.7824 + 0.3907(1 + Q^2/0.1422)^{-1}}{(1 + Q^2/0.5362)} F_2^\rho(Q^2) \\
&\quad + \kappa_{\rho'} \frac{g_{\rho'}}{f_{\rho'}} \frac{m_{\rho'}^2}{m_{\rho'}^2 + Q^2} F_2^\rho(Q^2) + \left(\kappa_\nu - 6.1731 N/2 - \kappa_{\rho'} \frac{g_{\rho'}}{f_{\rho'}}\right) F_2^D(Q^2) \\
F_1^{is}(Q^2) &= \frac{g_\omega}{f_\omega} \frac{m_\omega^2}{m_\omega^2 + Q^2} F_1^\omega(Q^2) + \frac{g_{\omega'}}{f_{\omega'}} \frac{m_{\omega'}^2}{m_{\omega'}^2 + Q^2} F_1^\omega(Q^2) + \frac{g_\phi}{f_\phi} \frac{m_\phi^2}{m_\phi^2 + Q^2} F_1^\phi(Q^2) \\
&\quad + \left(1 - \frac{g_\omega}{f_\omega} - \frac{g_{\omega'}}{f_{\omega'}}\right) F_1^D(Q^2) \\
F_2^{is}(Q^2) &= \kappa_\omega \frac{g_\omega}{f_\omega} \frac{m_\omega^2}{m_\omega^2 + Q^2} F_2^\omega(Q^2) + \kappa_{\omega'} \frac{g_{\omega'}}{f_{\omega'}} \frac{m_{\omega'}^2}{m_{\omega'}^2 + Q^2} F_2^\omega(Q^2) + \kappa_\phi \frac{g_\phi}{f_\phi} \frac{m_\phi^2}{m_\phi^2 + Q^2} F_2^\phi(Q^2) \\
&\quad + \left(\kappa_s - \kappa_\omega \frac{g_\omega}{f_\omega} - \kappa_{\omega'} \frac{g_{\omega'}}{f_{\omega'}} - \kappa_\phi \frac{g_\phi}{f_\phi}\right) F_2^D(Q^2)
\end{aligned} \tag{6}$$

where the pole terms are those of the ρ , ρ' , ω , ω' , and ϕ mesons, and the final term of each equation is determined by the asymptotic properties of PQCD. The F_i^α , $\alpha = \rho, \omega$, or ϕ are the meson-nucleon form factors, while the F_i^D are effectively quark-nucleon form factors.

For GKex the above hadronic form factors are parameterized in the following way:

$$\begin{aligned}
F_1^{\alpha,D}(Q^2) &= \frac{\Lambda_{1,D}^2}{\Lambda_{1,D}^2 + \tilde{Q}^2} \frac{\Lambda_2^2}{\Lambda_2^2 + \tilde{Q}^2} \\
F_2^{\alpha,D}(Q^2) &= \frac{\Lambda_{1,D}^2}{\Lambda_{1,D}^2 + \tilde{Q}^2} \left(\frac{\Lambda_2^2}{\Lambda_2^2 + \tilde{Q}^2} \right)^2
\end{aligned}$$

where $\alpha = \rho, \omega$ and $\Lambda_{1,D}$ is Λ_1 for F_i^α , Λ_D for F_i^D ,

$$\begin{aligned}
F_1^\phi(Q^2) &= F_1^\alpha \left(\frac{Q^2}{\Lambda_1^2 + Q^2} \right)^{1.5}, \quad F_1^\phi(0) = 0 \\
F_2^\phi(Q^2) &= F_2^\alpha \left(\frac{\Lambda_1^2 Q^2 + \mu_\phi^2}{\mu_\phi^2 \Lambda_1^2 + Q^2} \right)^{1.5} \\
\text{with } \tilde{Q}^2 &= Q^2 \frac{\ln[(\Lambda_D^2 + Q^2)/\Lambda_{\text{QCD}}^2]}{\ln(\Lambda_D^2/\Lambda_{\text{QCD}}^2)}.
\end{aligned} \tag{7}$$

This parameterization, together with Eq. (6), guarantees that the normalization conditions of Eq. (2) are met and that asymptotically

$$\begin{aligned}
F_1^i &\sim [Q^2 \ln(Q^2/\Lambda_{\text{QCD}}^2)]^{-2} \\
F_2^i &\sim F_1^i/Q^2 \\
i &= is, iv
\end{aligned} \tag{8}$$

as required by PQCD. The form factor $F_1^\phi(Q^2)$ vanishes at $Q^2 = 0$, and it and $F_2^\phi(Q^2)$ decrease more rapidly at large Q^2 than the other meson form factors. This conforms to the Zweig rule imposed by the $s\bar{s}$ structure of the ϕ meson [2].

This model has at most 14 free parameters:

- (i) 8 couplings to the pole terms, the 4 g_m/f_m and the 4 κ_m for the ρ' , ω , ω' and ϕ mesons.
- (ii) 4 cut-off masses in the hadronic form factors, Λ_1 , Λ_2 , Λ_D , and μ_ϕ .
- iii) The mass determining the size of the logarithmic Q^2 behavior, Λ_{QCD} .
- iv) The normalization factor N for the dispersion relation contribution of the ρ meson.

However at most 12 of these parameters are freely varied in any of the fits made in the next section to the chosen data sets.

III. DATA BASE AND FITTING PROCEDURE

As previously stated, GKex(01) is the same as DR-GK'(1) of [1]. This model had the best fit to the full data set available at the publication of [1] with $g'_\omega/f'_\omega = \kappa'_\omega = 0$ and with N=1. For GKex(01-) the 4 data points of [6] were omitted from that data set. In this case g'_ω/f'_ω and κ'_ω were still suppressed but N was freely varied.

In the fits GKex(02L) and GKex(02S) g'_ω/f'_ω and κ'_ω were freely varied, but these fits fixed N=1 again (implying negligible error in the dispersion relation evaluation) and Λ_{QCD} was fixed at the physical value of 0.15 GeV/c. The important difference from the data set of GKex(01-) is the addition of the higher Q R_p data points of [13] and the R_n data points of [14] and the omission of the G_{En} values for $Q^2 \geq 0.779$ GeV²/c² of [9], [18] and [17]. In the shorter data set of GKex(02S) the G_{Ep} values for $Q^2 \geq 1.75$ GeV²/c² of [7] are also omitted. The free parameters were optimized using a Mathematica program that incorporates the Levenberg-Marquardt method.

IV. RESULTS

Table I presents the parameters which minimize χ^2 for the above 4 cases. For all 4 parameter sets the hadronic form factor cut-off masses, Λ_1 , Λ_2 , Λ_D , and μ_ϕ . are reasonable. The relatively large value of Λ_2 , which controls the spin-flip suppression in QCD, is consistent with the slow approach to asymptopia observed in polarized hadron scattering. For the two cases in which Λ_{QCD} is a fitted parameter, as well as the two for which it is fixed, it is consistent with high energy experiment. The addition of the $\omega'(1.419)$ meson in GKex(02L) and GKex(02S) has moved κ_ω closer to the expected small negative value than all earlier fits, but there is still the implication of some effect from a higher mass isoscalar meson. The adequacy of the fits is an indication that the form factors with more poles would be similar to those already obtained.

In Table II the values of χ^2 are listed for the 4 cases and the contribution from each of the six form factor classes of measurement are detailed. Also shown are the values of χ^2 when any data points omitted from the fit are re-inserted.

We note, as can also be seen in Figs. 3 and 4 that the quality of fit to the magnetic form factors, G_{Mp} and G_{Mn} changes negligibly as we refit to the data sets that differ in the

TABLE I: Model parameters. Common to all models are $\kappa_v = 3.706$, $\kappa_s = -0.12$, $m_\rho = 0.776$ GeV, $m_\omega = 0.784$ GeV, $m_\phi = 1.019$ GeV, $m_{\rho'} = 1.45$ GeV and $m_{\omega'} = 1.419$ GeV.

Parameters	Models			
	GKex(01)	GKex(01-)	GKex(02L)	GKex(02S)
$g(\rho')/f(\rho')$	0.0636	0.0598	0.0608	0.0401
$\kappa(\rho')$	-0.4175	-15.9227	5.3038	6.8190
g_ω/f_ω	0.7918	0.6981	0.6896	0.6739
κ_ω	5.1109	1.9333	-2.8585	0.8762
g_ϕ/f_ϕ	-0.3011	-0.5270	-0.1852	-0.1676
κ_ϕ	13.4385	2.3241	13.0037	7.0172
μ_ϕ	1.1915	1.5113	0.6848	0.8544
$g(\omega')/f(\omega')$			0.2346	0.2552
$\kappa(\omega')$			18.2284	1.4916
Λ_1	0.9660	1.1276	0.9441	0.9407
Λ_D	1.3406	1.8598	1.2350	1.2111
Λ_2	2.1382	1.2255	2.8268	2.7891
Λ_{QCD}	0.1163	0.1315	0.150 ^(a)	0.150 ^(a)
N	1.0 ^(a)	0.8709	1.0 ^(a)	1.0 ^(a)

^(a)not varied

TABLE II: Contributions to the standard deviation, χ^2 , from each data type for each of the models. The number of data points contributing is in parentheses. For each data type the first row corresponds to the data set for which the model parameters were optimized, the second row to the full data set.

Data type	Data set	Models			
		GKex(01)	GKex(01-)	GKex(02L)	GKex(02S)
G_{Mp}	opt	43.3(68)	43.6(68)	48.1(68)	47.9(68)
	full	same as above			
G_{Ep}	opt	67.2(48)	48.2(44)	75.3(44)	30.5(36)
	full	67.2(48)	74.8(48)	112.2(48)	136.8(48)
G_{Mn}	opt	122.4(35)	120.2(35)	121.0(35)	122.7(35)
	full	same as above			
G_{En}	opt	64.8(23)	64.2(23)	24.1(15)	24.2(15)
	full	65.3(24)	65.0(24)	68.2(24)	68.3(24)
R_p	opt	29.0(17)	22.6(17)	23.1(21)	11.8(21)
	full	114.0(21)	106.5(21)	23.1(21)	11.8(21)
R_n	opt	0.0(0)	0.0(0)	0.6(3)	0.6(3)
	full	9.6(3)	17.7(3)	0.6(3)	0.6(3)
Total	opt	326.7(191)	298.9(187)	336.3(195)	237.7(178)
	full	421.8(199)	427.8(199)	369.2(199)	388.1

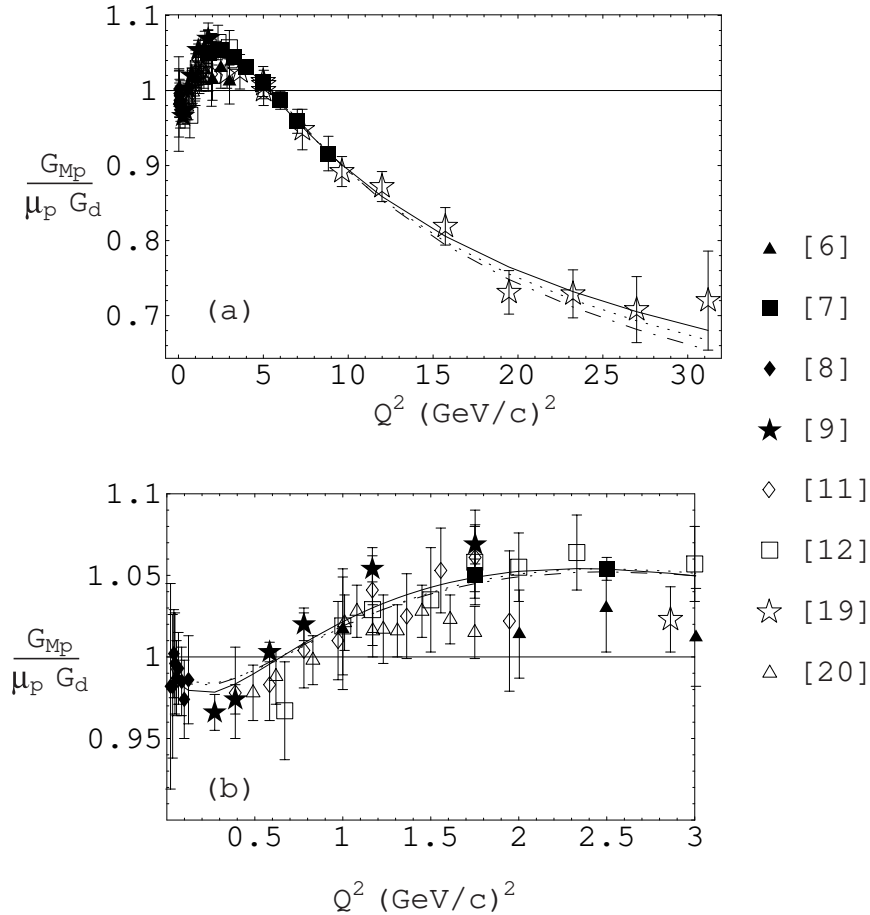


FIG. 3: G_{Mp} normalized to $\mu_p G_d$. Comparison of the models GKex(01) [solid], GKex(02L) [dotted] and GKex(02S) [dash-dotted] with the data of [6], [7], [8], [9], [11], [12], [19] and [20]. (a) The full data range. (b) Expansion of the range $Q^2 \leq 3.0 \text{ GeV}^2/c^2$. The data symbols are listed in the figure.

electric form factors and the electric to magnetic form factor ratios. As discussed in [1], the large excess of χ^2 over the number of data points for G_{Mn} is due to obvious inconsistencies in the data set for G_{Mn} at $Q^2 < 0.8 \text{ GeV}^2/c^2$. The displacement of adjacent data points well beyond their error bars in this range is evident in the figures and contributes about 90 to the χ^2 of G_{Mn} .

The interesting changes are, of course, in the fits to G_{Ep} , G_{En} , R_p and R_n . As noted in the introduction, removing the 4 very high values of G_{Ep} data [6] does surprisingly little to allow a better fit to the R_p data already in GKex(01). Several of the parameters, all three κ_m , Λ_2 and Λ_D , have large changes (see Table I), but this results in a small shift between the predictions of GKex(01 and GKex(01-) as is evident in Table II and Figs. 1 and 2. The figures show a slightly better fit to R_p correlated with a very slightly worse fit to G_{Ep} . The former is reflected in Table II by the decrease in the χ^2 contribution of the 17 R_p points to which those cases were optimized from 29.0 to 22.6. When the 4 higher Q^2 of [13] are added the χ^2 contribution is much larger than the number of points (21). The drop in the χ^2 contribution to G_{Ep} from 67.2 to 48.2 is entirely due to the omission of the 4 data points

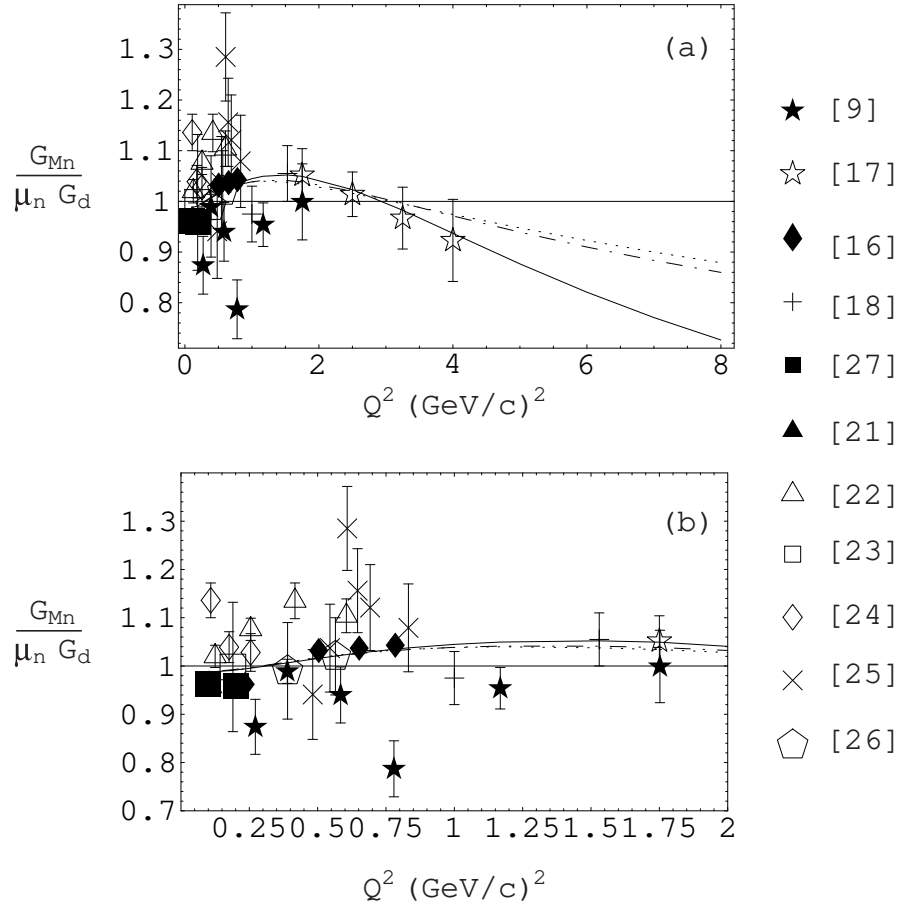


FIG. 4: G_{Mn} normalized to $\mu_n G_d$. Comparison of the models GKex(01) [solid], GKex(02L) [dotted] and GKex(02S) [dash-dotted] with the data of [9], [16], [17], [18], [21], [22], [23], [24], [25], [26], and [27]. The data symbols are listed in the figure. (a) The full data range. (b) Expansion of the range $Q^2 \leq 2.0 \text{ GeV}^2/c^2$.

of [6], but the χ^2 for the full set of 48 points is a little larger because of the competition with R_p . The implication is that there is a constraint on the fit to R_p from data independent of G_{Ep} , arising from the model correlations between all the nucleon emff. This is shown to be the case below.

Substituting the new R_n values for the conflicting G_{En} data of [9], [17] and [18] causes a large difference between the GKex(02L) and GKex(01-) fits to G_{Ep} , G_{En} , R_p and R_n , as seen in Table II and Fig. 5 - Fig. 8. In particular for GKex(02L) the χ^2 contribution for all 21 R_p data points is 23.1. Fig. 6 shows the strong improvement in the fit to R_p . The figure also shows that the goodness of the χ^2 value is somewhat misleading because that fit is systematically high for the 3 highest Q^2 data points. On the other hand the χ^2 contribution for all 44 G_{Ep} data points increases from 48.2 in GKex(01-) to 75.3 in GKex(02L) because of the compromise of better fitting R_p . The χ^2 contribution for the 3 R_n points now included is only 0.6. G_{En} now contributes 24.1 for the remaining 15 data points (which still include highly scattered low Q^2 data as discussed in [1]) instead of 64.8 for the 23 data points in GKex(01-).

For the GKex(02S) case the G_{Ep} data of [7], which is clearly inconsistent with the new

R_p data [5] and [13], is also omitted. The results are very good if the modern data is chosen when in conflict with the older Rosenbluth separation results. The χ^2 contribution from the remaining 36 G_{Ep} points is only 30.6 and for all 21 R_p points only 11.8. For the remaining types of form factor measurements there is a negligible change of χ^2 between the GKex(02L) and GKex(02S) cases.

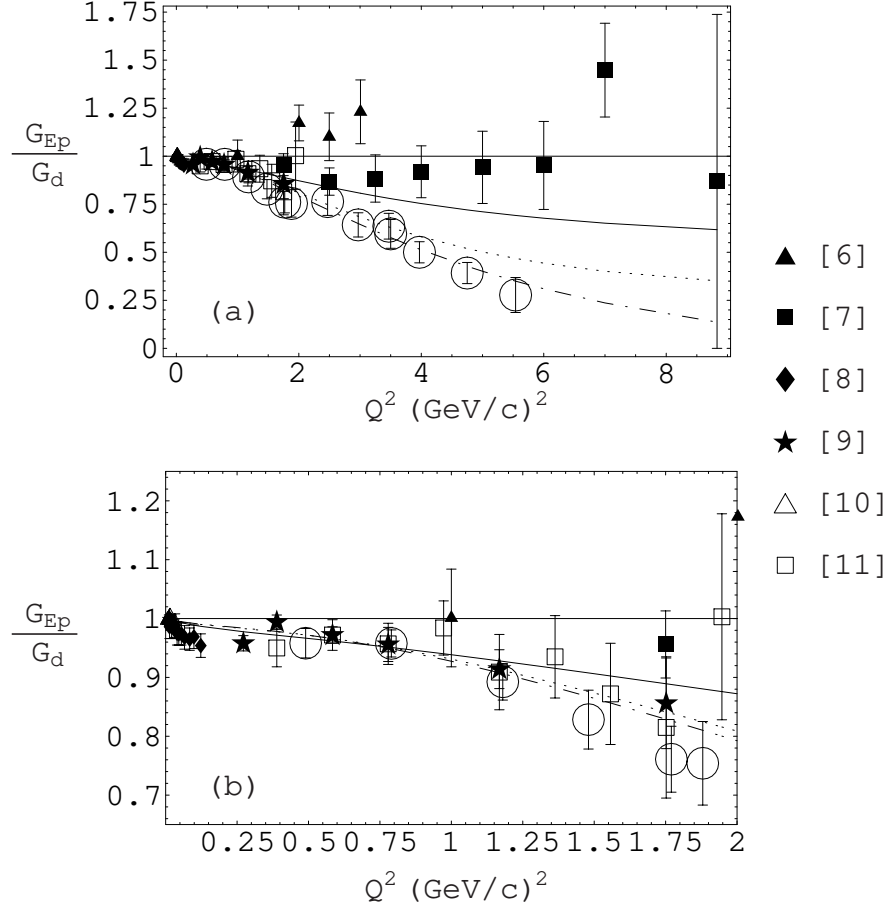


FIG. 5: G_{Ep} normalized to G_d . Comparison of the models GKex(01) [solid], GKex(02L) [dotted] and GKex(02S) [dash-dotted] with the data. The data references are the same as in Fig. 1 and the data symbols are listed in the figure. The points labelled by open circles are obtained by multiplying R_p data [5] and [13] by the G_{Mp} of GKex(02S) normalized by $\mu_p G_d$. (a) The full data range. (b) Expansion of the range $Q^2 \leq 2.0 \text{ GeV}^2/c^2$.

Figs. 5, 6, 7, and 8 show the successive improvements in G_{Ep} , R_p , G_{En} , and R_n as the optimization data sets are varied from GKex(01) to GKex(02L) and to GKex(02S). To demonstrate the correlation between the electric form factors and the ratio of electric to magnetic form factors we have, in Figs. 5 and 7, entered (as circles) the electric form factor values obtained by multiplying the experimental R_p and R_n values by the case GKex(02S) model values of the magnetic form factors normalized by the magnetic moments. The correlation with the model prediction for the electric form factors is excellent.

The figures show the model extrapolations of R_p , G_{Mn} , G_{En} and R_n up to Q^2 of $8 \text{ GeV}^2/c^2$ for the guidance of future experiments and because of their relevance to deuteron and other

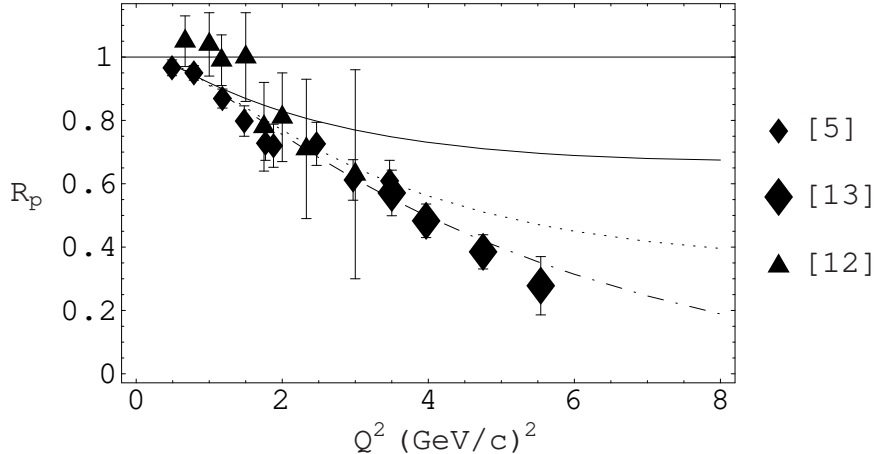


FIG. 6: R_p , the ratio $\mu_p G_{Ep}/G_{Mp}$. Comparison of the models GKex(01) [solid], GKex(02L) [dotted] and GKex(02S) [dash-dotted] with the data. The data is from [5], [12], and [13].

nuclear electromagnetic scattering predictions. The extrapolation is sensitive to the weight given to the polarized vs. the Rosenbluth separation data in the fits. The resolution of this dichotomy will, in the context of the physical model employed here, greatly restrict the nucleon emff over a large range of momentum transfer.

The polarization measurements of R_p and R_n may soon be extended to larger Q^2 , so it is of interest to examine the predictions of the good fit GKex(02S) as Q^2 increases. As seen in Fig. 5 the model curve is, as is the data, approximately linear in the range $0.5 \text{ GeV}^2/c^2 \leq Q^2 \leq 5.6 \text{ GeV}^2/c^2$, but the model curve's slope is gradually decreasing in magnitude. A linear fit to the data would change sign near $Q^2 = 8 \text{ GeV}^2/c^2$ where the model predicts 0.19. The model crosses zero near $Q^2 = 14 \text{ GeV}^2/c^2$ with a very small slope.

Fig. 8 shows the Galster curve, $R_n^{Galster}(Q^2)$ of Eq. (1), to compare with the model and the data. The model fits the data but deviates from the Galster curve after that. The model increases faster, reaching a maximum of 0.426 at $Q^2 = 4 \text{ GeV}^2/c^2$ where the Galster value is only 0.309, while $R_n^{Galster}(Q^2)$ increases monotonically to an asymptotic value of 0.342. A measurement of the present quality at $Q^2 = 4 \text{ GeV}^2/c^2$ could distinguish between the two.

V. CONCLUSIONS

The GKex model, consistent with vector meson dominance and perturbative QCD in the appropriate momentum transfer regions, represents well a consistent set of neutron and proton emff. This set includes polarization measurements, which are directly related to the ratios of electric to magnetic form factors, and differential cross section measurements of the magnetic form factors. The values of the electric form factors from the Rosenbluth separation of the differential cross section is, in our final selection GKex(02S), only used for the lower range of Q^2 where the magnetic contributions are less dominant. Because of the physical properties of the model and the good quality of the fit we expect that the model predictions are sufficiently accurate to be used for predictions of the electromagnetic properties of nuclei. The model values may also be useful in planning future experiments.

The above conclusions are only valid to the extent that adequate physics is included

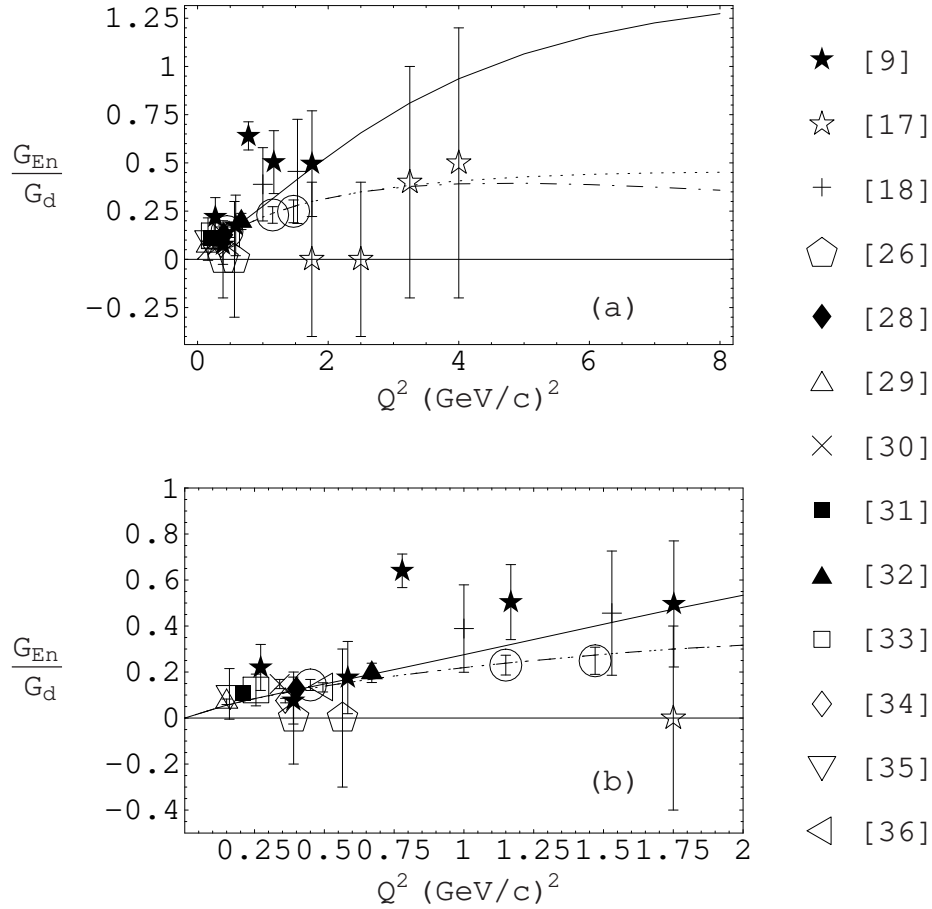


FIG. 7: G_{En} normalized to G_d . Comparison of the models GKex(01) [solid], GKex(02L) [dotted] and GKex(02S) [dash-dotted] with the data of [9], [17], [18], [26], [28], [29], [30], [31], [32], [33], [34], [35] and [36]. The data of [30], [32] and [34] are the reevaluated values of [37]. The slope at $Q^2 = 0$ is from [38]. The points labelled by open circles are obtained by multiplying R_n data [14] by the G_{Mn} of GKex(02S) normalized by $\mu_n G_d$. (a) $Q^2 \leq 8.0 \text{ GeV}^2/c^2$. (b) Expansion of the range $Q^2 \leq 2.0 \text{ GeV}^2/c^2$.

in the GKex models. Only the ρ meson exchange includes the width of the vector mesons (from dispersion relation results). There will be corrections from the widths of the other exchanged vector mesons. However the next most important, the ω and ϕ , have very narrow widths. The higher masses of the ρ' (1450) and the ω' (1420) reduces the importance of their substantial widths because of their distance from the physical region and their partial replacement by the pQCD term.

In assuming vector dominance we have neglected the multi-meson exchange continuum contributions. In particular the two-pion continuum may have an influence at very low $Q^2 \leq 0.4 \text{ GeV}^2/c^2$. Indeed, as remarked in [1] and can be seen in Fig. 5b, the G_{Ep} data of [8] has a more negative slope for $Q^2 \leq 0.3 \text{ GeV}^2/c^2$ than the higher Q^2 data and the model fit. The addition of a 2-pion exchange term to the model may enable a change of slope between the two regions, but would have little effect on the model fit for $Q^2 \geq 0.5 \text{ GeV}^2/c^2$.

One may also want to consider some higher mass vector mesons. This would have some

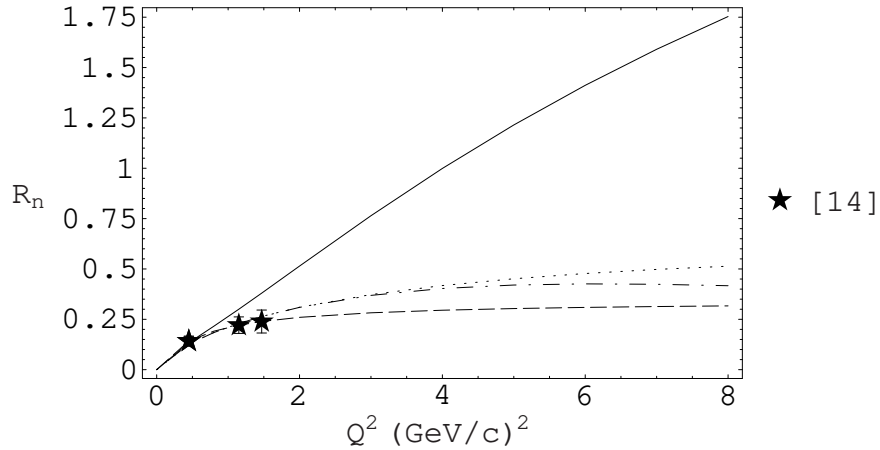


FIG. 8: R_n , the ratio $\mu_n G_{En}/G_{Mn}$. Comparison of the models GKex(01) [solid], GKex(02L) [dotted] and GKex(02S) [dash-dotted] with the data. The dashed curve is $R_n^{Galster}(Q^2)$ of Eq. (1). The “experimental” points are described in the text [14].

importance in the fits of [3] and [4], but are much less important in these GK type models because of the transition to pQCD behavior.

Acknowledgments

The author is grateful to Charles Perdrisat and Richard Madey for timely information about their polarization measurements.

-
- [1] Earle L. Lomon, Phys. Rev. **C64**, 035204 (2001).
 - [2] M.F. Gari and W. Krümpelmann, Phys. Lett. **B274**, 159 (1992); erratum, Phys. Lett. **B282**, 483 (1992).
 - [3] P. Mergell, Ulf-G. Meissner and D. Drechsel, Nucl. Phys. **A596**, 367 (1996).
 - [4] G. Höhler et al., Nucl. Phys. **B114**, 505 (1976).
 - [5] M.K. Jones et al., Phys. Rev. Lett. **84**, 1398 (2000).
 - [6] R.C. Walker et al., Phys. Rev. **D49**, 5671 (1994).
 - [7] L. Andivahis et al., Phys. Rev. **D50**, 5491 (1994).
 - [8] F. Borkowski et al., Nucl. Phys. **B93**, 461 (1975).
 - [9] K.M. Hanson et al., Phys. Rev. **D8**, 753 (1973).
 - [10] J.J. Murphy et al., Phys. Rev. **C9**, 2125 (1974).
 - [11] C.H. Berger et al., Phys. Lett. **35B**, 87 (1971).
 - [12] W. Bartel et al., Nucl. Phys. **B58**, 429 (1973).
 - [13] O. Gayou et al. Phys. Rev. Lett. **88**, 092301 (2002).
 - [14] Richard Madey, private communication; Bull. APS**46**, DB 10, p 34, Oct. 2001.
 - [15] S. Galster et al., Nucl. Phys. **B32**, 221 (1971).
 - [16] H. Anklin et al., Phys. Lett. **B428**, 248 (1998).

- [17] A. Lung et al., Phys. Rev. Lett. **70**, 718 (1993).
- [18] W. Bartel et al., Phys. Lett. **B39**, 407 (1972).
- [19] A.F. Sill et al., Phys. Rev. **D48**, 29 (1993).
- [20] P.E. Bosted et al., Phys. Rev. **C42**, 38 (1990).
- [21] H. Anklin et al., Phys. Lett. **B336**, 313 (1994).
- [22] E.E.W. Bruins et al., Phys. Rev. Lett. **75**, 21 (1995).
- [23] H. Gao et al., Phys. Rev. **C50**, R546 (1994).
- [24] P. Markowitz et al., Phys. Rev. **C48**, R5 (1993).
- [25] A.S. Esauslov et al., Yad. Fiz. **45**, 410 (1987) [Sov. J. Nucl. Phys. **45**, 258 (1987)].
- [26] W. Bartel et al., Phys. Lett. **30B**, 285 (1969).
- [27] W. Xu et al., Phys. Rev. Lett. **85**, 2900 (2000).
- [28] J. Golak et al., Phys. Rev. **C63**, 1034006 (2001).
- [29] C. Herberg et al., Eur. Phys. J. **A5**, 131 (1999).
- [30] M. Ostrick et al., Phys. Rev. Lett. **83**, 276 (1999).
- [31] I. Passchier et al., Phys. Rev. Lett. **82**, 4988 (1999).
- [32] D. Rohe et al., Phys. Rev. Lett. **83**, 4257 (1999).
- [33] T. Eden et al., Phys. Rev. **C50**, R1749 (1994).
- [34] M. Meyerhoff et al., Phys. Lett. **B327**, 201 (1994).
- [35] C.E. Jones-Woodward et al., Phys. Rev. **C44**, R571 (1999).
- [36] H. Zhu et al., Phys. Rev. Lett. **87**, 081801 (2001).
- [37] T. Walcher (private communication).
- [38] S. Kopecky et al., Phys. Rev. Lett. **74**, 2427 (1995).